

# One-parameter superscaling in three dimensions

János Pipek<sup>a</sup> Imre Varga<sup>a,b\*</sup> and Etienne Hofstetter<sup>c</sup>

<sup>a</sup>Elméleti Fizika Tanszék, Budapesti Műszaki és Gazdasagtudományi Egyetem,  
H-1521 Budapest, Hungary

<sup>b</sup>Fachbereich Physik, Philipps–Universität Marburg,  
Renthof 6, D-35032 Marburg an der Lahn, Germany

<sup>c</sup>Management School, Imperial College, London SW7 2BX, United Kingdom

---

## Abstract

Numerical and analytical details are presented on the newly discovered superscaling property of the energy spacing distribution in the three dimensional Anderson model.

*PACS:* 71.30.+h, 72.12.Rn, 05.40.+j .

*Keywords:* spacing distribution, random matrix theory, Anderson localization, metal–insulator transition.

---

## 1. Introduction

The statistical properties of the spectra of disordered systems continues to be a vivid field of research both analytically and numerically. It is by now well established that the spectral fluctuations in the limit of vanishing disorder are described by the random matrix theory (RMT) [1,2] with corrections of the order of  $1/g$ , where  $g$  is the dimensionless classical conductance of the system. This is because in this regime the states are extended (ergodic). In the limit of infinite disorder, on the other hand, due to the extremely strong localization of the eigenstates the levels are practically uncorrelated at least in the thermodynamic limit.

The first attempts [3] to investigate the statistics at the localization–delocalization transition (LDT) (also known as the metal–insulator transition), showed that indeed the statistics at the LDT is different from the two other extremes. Eventually it shares some of the features of both of them. It has been shown numerically in many simulations [3–8] that e.g. the nearest neighbor

spacing distribution,  $P(s)$ , the probability of finding no eigenlevels within an energy window of length  $s$ , behaves for low- $s$  as  $P(s) \sim s^\beta$ , and for large- $s$  as  $\ln P(s) \sim -as$ , where  $\beta = 1, 2$  and  $4$  depending on the global orthogonal, unitary and symplectic symmetry of the system, and  $a$  is a constant that depends weakly on  $\beta$  but strongly on dimensionality  $d$  [4–6]. The presence of the level repulsion at low- $s$  is a direct consequence that the eigenstates at the LDT are heavily fluctuating but still strongly overlapping [9]. The heavy fluctuations expressed as their multifractal character [10] enters in the parameter  $a$  that is connected both to the correlation dimension of the states and the level compressibility [11]. Such a relation shows how the statistical properties of the levels and the states are coupled at the LDT.

In a previous publication [8] we have presented numerical evidence that using appropriate indices to describe the overall shape of  $P(s)$ , a superuniversal (i.e.  $\beta$  independent) scaling relation is revealed as the system undergoes the transition from the metal to an insulator. Here we give further evidence that with the change of system size  $L$  and disorder  $W$  the nearest neighbor spac-

---

\*Supported by OTKA T029813, T032116 and F024135 and the Alexander von Humboldt foundation

ing distribution,  $P(s)$ , evolves as a one-parameter family of distributions. A similar evolution has been shown analytically to exist by Shapiro [12] for the conductance distribution in  $d = 2 + \varepsilon$ . The parameter in our case is also the scaling variable that can be chosen as  $g$ , i.e. the classical, dimensionless conductance of the system.

## 2. The model and the analysis

In order to study the statistical properties of disordered systems with and without time reversal symmetry and with broken rotational symmetry we have used the Anderson model which is a tight-binding model defined on a  $L^3$  lattice. For the details we refer to the review of Kramer and MacKinnon [13] and also our previous work [8]. In Ref. [8] the numerical results have been illustrated using the symplectic case where the rotational symmetry has been broken with the introduction of spin-orbit scattering. Here we present the results of the case with (without) time reversal symmetry corresponding to the orthogonal (unitary) symmetry. Time reversal symmetry has been broken by the introduction of a magnetic field.

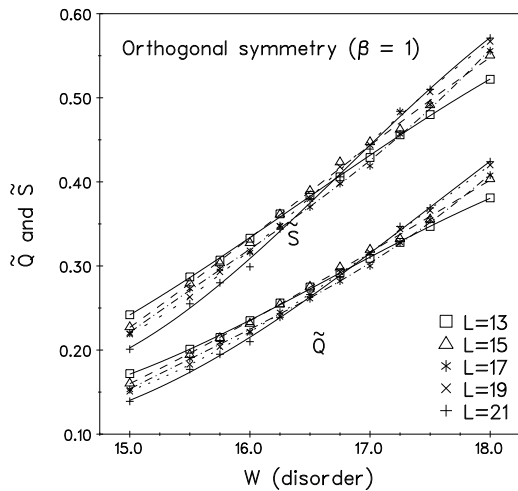


Figure 1.  $\tilde{Q}(L, W)$  and  $\tilde{S}(L, W)$  for the case of orthogonal symmetry. Continuous curves are polynomial fits.

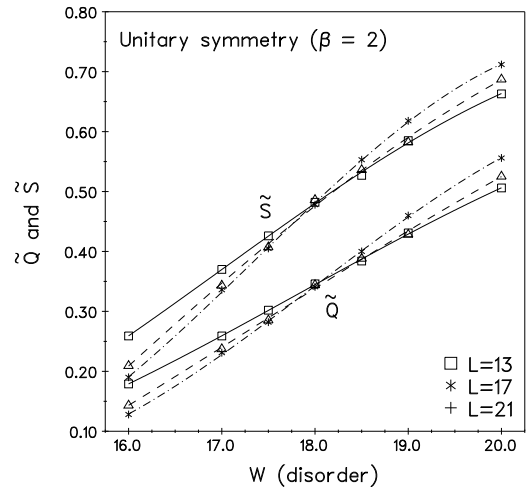


Figure 2.  $\tilde{Q}(L, W)$  and  $\tilde{S}(L, W)$  for the case of unitary symmetry. Continuous curves are polynomial fits.

After appropriately unfolding the spectra in many samples of the system we calculated the nearest neighbor spacing distribution,  $P(s)$ . For each system size  $L$  and disorder  $W$  the number of spacings was of the order of  $10^5$ . In order to characterize the shape of  $P(s)$  we use generalized Rényi-entropies [14]

$$q = \mu_2^{-1} \quad \text{and} \quad S_{str} = \mu_S + \ln \mu_2, \quad (1)$$

where  $\mu_2 = \langle s^2 \rangle$  is the second moment of  $P(s)$ , while  $\mu_S = -\langle s \ln s \rangle$ . After a proper rescaling we obtain

$$\begin{aligned} -\ln(q) &\rightarrow \frac{-\ln(q) + \ln(q_W)}{-\ln(q_P) + \ln(q_W)} = \tilde{Q} \\ S_{str} &\rightarrow \frac{S_{str} - S_W}{S_P - S_W} = \tilde{S} \end{aligned} \quad (2)$$

where index  $P$  refers to the Poissonian, uncorrelated case and  $W$  to the Wigner-surmise representing the RMT cases respectively. Their values are listed in Table 1. Such a rescaling ensures that  $\tilde{S} = \tilde{Q} = 0(1)$  belonging to the RMT (Poisson) limit. In Figs. 1 and 2 we present the way how  $\tilde{S}$  and  $\tilde{Q}$  vary as a function of disorder for various system sizes. The scale invariance at around  $W = W_c$  shows the presence of the LDT.

In Table 2 we collected the values of the critical disorder and the critical exponent obtained

Table 1

Shape descriptive parameters for the case of different  $P(s)$  functions.

	Poisson	$\beta = 1$	$\beta = 2$	$\beta = 4$
$q$	0.5295	0.7854	0.8488	0.9054
$-\ln(q)$	0.6358	0.2416	0.1639	0.0994
$S_{str}$	0.2367	0.1025	0.0733	0.0464

from a linearization around this fixed point. Even though the values presented in Table 2 agree well with the ones known from earlier calculations, the precision is somewhat lower.

In Figure 3 we plot the  $\tilde{S}$  as a function of  $\tilde{Q}$  for all the symmetries ( $\beta = 1, 2$  and 4). As a comparison we also plotted our analytical estimates based on a phenomenological assumption and the relation obtained for the interpolating formula of Israilev [15]. We will show below evidence that

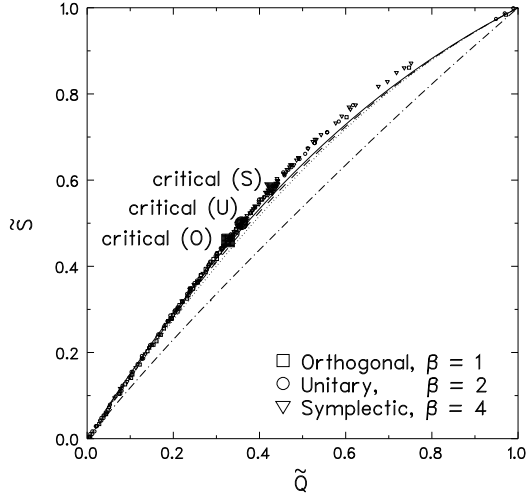


Figure 3.  $\tilde{S}(L, W)$  as a function of  $\tilde{Q}(L, W)$  for all the symmetry classes. The solid symbols represent the positions of the critical points. The continuous (solid, dashed, dotted) curves are our analytical estimates, see text for details. The dashed dotted line shows the relation of the  $P(s)$  due to Israilev [15] representing the pure effect of level repulsion.

the overall scaling behavior in Figure 3 can be understood if the spacing distribution for any finite

Table 2

Position of the critical point and critical exponents obtained using the shape descriptive parameters  $\tilde{Q}$  and  $\tilde{S}$ .

	$W_c$	$\nu$
$\beta = 1$ (O)	$16.77 \pm 0.63$	$1.30 \pm 0.38$
$\beta = 2$ (U)	$18.13 \pm 0.38$	$1.63 \pm 0.57$
$\beta = 4$ (S)	$21.97 \pm 0.17$	$1.41 \pm 0.32$

value of  $W$  and  $L$ , i.e. for  $0 < g < \infty$  is given as

$$\mathcal{P}_{g,\beta}(e^x) = \int_{-\infty}^{\infty} \mathcal{Q}_{g,\beta}(e^{x-y}) \mathcal{W}_{\beta}(e^y) dy \quad (3)$$

with  $e^x \equiv s$ . Here the function  $\mathcal{W}_{\beta}(t)$  is simply the Wigner–surmise and  $\mathcal{P}_{g,\beta}(s)$  is the histogram measured in the numerical simulation. All three functions,  $\mathcal{P}$ ,  $\mathcal{Q}$  and  $\mathcal{W}$  are spacing distribution functions.

In the next section we will prove that for the convolution of the type (3) the Rényi–entropies introduced in [14] are additive. Therefore, apart from the denominator, the constant shift in (2) corresponds to  $\mathcal{W}_{\beta}$  in (3), hence we may conclude that the relation in Figure 3 is described by the properties of function  $\mathcal{Q}$ .

We will also show that the solution of (3) for  $\mathcal{Q}_{g,\beta}(u)$  in the extreme cases ( $g = 0$  and  $g \rightarrow \infty$ ) can be done analytically and that a phenomenological interpolation can describe the  $\tilde{S}$  vs.  $\tilde{Q}$  relation in Figure 3.

### 3. Additivity of Rényi entropies

The expression (3) is in fact a convolution and after a variable transformation can be written as

$$\mathcal{P}_{g,\beta}(s) = \int_0^{\infty} \mathcal{Q}_{g,\beta}\left(\frac{s}{t}\right) \mathcal{W}_{\beta}(t) \frac{dt}{t}. \quad (4)$$

Let us denote the  $k$ -th moment of a distribution  $\mathcal{F}$  by  $\mu_k[\mathcal{F}]$ . Then it is easy to see from (4) (omitting indices  $g$  and  $\beta$ ) that

$$\begin{aligned} \mu_k[\mathcal{P}] &= \int_0^{\infty} ds s^k \mathcal{P}(s) \\ &= \int_0^{\infty} \frac{dt}{t} \mathcal{W}(t) \int_0^{\infty} ds s^k \mathcal{Q}\left(\frac{s}{t}\right) \\ &= \int_0^{\infty} dt t^k \mathcal{W}(t) \int_0^{\infty} du u^k \mathcal{Q}(u) \end{aligned}$$

$$= \mu_k[\mathcal{W}]\mu_k[\mathcal{Q}], \quad (5)$$

which for  $g = -\ln \mu_2$  yields the desired additivity. A similar procedure yields the additivity of the quantity  $S_{str}$ . The key step is to realize that the entropic moment of  $\mathcal{F}$  is  $\mu_S[\mathcal{F}] = \langle s \ln s \rangle$  which can be expressed as

$$\mu_S[\mathcal{P}] = \mu_1[\mathcal{Q}]\mu_S[\mathcal{W}] + \mu_1[\mathcal{W}]\mu_S[\mathcal{Q}]. \quad (6)$$

#### 4. Phenomenological approximation

Here we show that the solution of (3) for  $\mathcal{Q}_{g,\beta}(u)$  in the extreme cases ( $g = 0$  and  $g \rightarrow \infty$ ) can be obtained analytically and that a phenomenological interpolation can describe the  $\tilde{S}$  vs.  $\tilde{Q}$  relation in Figure 3. First it is easy to see that for the case of vanishing disorder ( $g \rightarrow \infty$ ) we expect that  $\mathcal{P}(s) \rightarrow \mathcal{W}(s)$ . In this case  $\mathcal{Q}(u) = \delta(u - 1)$ . On the other hand at the other extreme, when  $g \rightarrow 0$ , another universality is expected:  $\mathcal{P}(s) \rightarrow \exp(-s)$ , the Poissonian distribution. In this case after nontrivial calculations, Eq. (4) is solved for  $\mathcal{Q}_{0,\beta}(s) \equiv R(bs)$

$$R(y) = a \begin{cases} e^{-y^2} & \text{(O)} \\ \text{erfc}(y) & \text{(U)} \\ (2y^2 + 1)\text{erfc}(y) - \frac{2y}{\sqrt{\pi}}e^{-y^2} & \text{(S)} \end{cases} \quad (7)$$

where  $y = bs$ , with  $b = 1/\sqrt{\pi}$ ,  $\sqrt{\pi}/4$ , and  $3\sqrt{\pi}/16$  and  $a = 2/\pi$ ,  $\pi/4$ , and  $9\pi/32$  for  $\beta = 1, 2$  and  $4$ , respectively. The complementary error function is denoted as  $\text{erfc}$ . Now a phenomenological step is introduced in order to describe the evolution of  $\mathcal{P}$  for any finite value of  $g$ . We propose a simple form

$$\mathcal{Q}_{g,\beta}(s) = a_{g,\beta}s^g R(b_{g,\beta}s) \quad (8)$$

where the coefficients  $a_{g,\beta}$  and  $b_{g,\beta}$  are determined from the normalization conditions  $\mu_0[\mathcal{Q}] = \mu_1[\mathcal{Q}] = 1$ . Obviously for  $g \rightarrow 0$  they yield the values given above for (7). For  $g \rightarrow \infty$   $\mathcal{Q}(s) \rightarrow \delta(s - 1)$ , as well. The  $\tilde{S}$  vs.  $\tilde{Q}$  relation for this interpolating function is depicted as continuous curves in Fig. 3. They still have a small  $\beta$  dependence but follow the data very closely. The  $\beta$ -dependence can be attributed to (i) the simple interpolation we used in (8) and to (ii) the fact that we focused only on the linear shift introduced in (2) and disregarded the denominator.

#### 5. Conclusion

In this paper we have given further details, both numerical and analytical of a recently discovered scaling relation existing in the evolution of the nearest neighbor spacing distribution,  $P(s)$ , as the dimensionless conductance  $g$  changes from 0 (localized) to  $\infty$  (metal).

#### REFERENCES

1. M.L. Mehta, *Random Matrices* (Academic Press, Boston, 1991).
2. T. Guhr, A. Müller-Groeling, and H.A. Weidenmüller, Phys. Rep. **299**, 189 (1998).
3. B.L. Shklovskii, B. Shapiro, B.R. Sears, P. Lambrianides, and H.B. Shore, Phys. Rev. **B47**, 11487 (1993).
4. I.Kh. Zharekeshev and B.Kramer, Phys. Rev. Lett. **79**, 717 (1997).
5. M.Batsch, L. Schweitzer, I.Kh. Zharekeshev, and B. Kramer, Phys. Rev. Lett. **77**, 1552 (1996).
6. T. Kawarabayashi, T. Ohtsuki, K. Slevin, and Y. Ono, Phys. Rev. Lett. **77**, 3593 (1996).
7. D. Braun, G. Montambaux, and M. Pascaud, Phys. Rev. Lett. **81**, 1062 (1998).
8. I. Varga, E. Hofstetter, and J. Pipek, Phys. Rev. Lett. **82**, 4683 (1999).
9. Y.V. Fyodorov and A.D. Mirlin, Phys. Rev. **B55**, R16001 (1997).
10. M. Janssen, Phys. Rep. **295**, 1 (1998).
11. J.T. Chalker, I.V. Lerner, and R.A. Smith, Phys. Rev. Lett. **77**, 554 (1996); J.T. Chalker, V.E. Kravtsov, and I.V. Lerner, Pis'ma Zh. Eksp. Teor. Fiz. B. **82** 295 (1996).
12. B. Shapiro, Phys. Rev. **B34**, 4394 (1986); Philos. Mag. **56**, 1031 (1987).
13. B. Kramer and A. MacKinnon, Rep. Prog. Phys. **56**, 1469 (1993) and references therein.
14. I. Varga, *et al.* Phys. Rev. **B52**, 7783 (1995); see also J. Pipek and I. Varga, Phys. Rev. **A46**, 3148 (1992)
15. F. Izrailev, J. Phys. A: Math. Gen **22**, 865 (1989).